


A Likelihood Ratio Detector for QTMS Radar and Noise Radar

DAVID LUONG , Graduate Student Member, IEEE
Carleton University, Ottawa, ON, Canada

BHASHYAM BALAJI , Senior Member, IEEE
Defence Research and Development Canada, Ottawa, ON, Canada

SREERAMAN RAJAN , Senior Member, IEEE
Carleton University, Ottawa, ON, Canada

We derive a detector function for quantum two-mode squeezing (QTMS) radar and noise radar that is based on the use of a generalized likelihood ratio (GLR) test for distinguishing between the presence and absence of a target. In addition to an explicit expression for the GLR detector, we derive a detector function which approximates the GLR detector in the limit where the target is small, far away, or otherwise difficult to detect. When the number of integrated samples is large, we derive a theoretical expression for the receiver operating characteristic (ROC) curve of the radar when the GLR detector is used. When the number of samples is small, we use simulations to understand the ROC curve behavior of the detector. One interesting finding is that there exists a parameter regime in which a previously-studied detector outperforms the GLR detector, contrary to the intuition that LR-based tests are optimal or nearly so. This is because neither the Neyman–Pearson lemma, nor the Karlin–Rubin theorem which generalizes the lemma to composite hypotheses, hold in this particular problem. However, the GLR detector remains a good choice for target detection in certain regimes.

Manuscript received July 24, 2021; revised November 18, 2021 and January 5, 2022; released for publication January 8, 2022. Date of publication January 25, 2022; date of current version August 9, 2022.

DOI. No. 10.1109/TAES.2022.3145296

Refereeing of this contribution was handled by Y. D. Zhang. (*Corresponding author: David Luong.*)

This work was supported by the Natural Science and Engineering Research Council of Canada (NSERC). The work of David Luong was supported by the Vanier scholarship.

Authors' addresses: David Luong and Sreeraman Rajan are with Carleton University, Ottawa, ON K1S 5B6, Canada, E-mail: (david.luong3@carleton.ca; sreeramanr@sce.carleton.ca); Bhashyam Balaji is with Defence Research and Development Canada, Ottawa, ON K2K 2Y7, Canada, E-mail: (bhashyam.balaji@drdc-rddc.gc.ca).

This work is licensed under a Creative Commons Attribution 4.0 License. For more information, see <https://creativecommons.org/licenses/by/4.0/>

I. INTRODUCTION

From an abstract mathematical perspective, radars are machines for hypothesis testing: they decide whether a target is present or absent [1]. The physical operation of the radar dictates the exact nature of the test: what distributions the radar detection data are drawn from, which statistics are being used, and—most importantly—how powerful the test is. In fact, the gold standard for analyzing the detection performance of any radar is the *receiver operating characteristic* (ROC) curve, which gives the probability of detection as a function of the probability of false alarm. That is to say, the ROC curve is the power of the hypothesis test performed by the radar as a function of the significance level. Therefore, when trying to understand how well a given radar works, a careful analysis of the hypothesis testing performed by the radar is fundamental.

In this article, we are concerned with a class of radars known as *noise radars* [2]–[12]. This type of radar generates a pair of correlated electromagnetic noise signals, of which one is sent at a target and the other is retained as a reference signal within the radar. There is a very important subclass of radars which comes under the umbrella of noise radar, namely *quantum two-mode squeezing* (QTMS) radar. As the name implies, QTMS radar is a type of quantum radar, a variant of *quantum illumination* [13]–[16]. QTMS radar was the first type of microwave quantum radar for which a laboratory prototype has been built and the results published in scientific publications [17]–[20]. From the point of view of target detection, it has been shown that noise radars and QTMS radars effectively lie on a continuum characterized by the correlation coefficient between the signal received by a radar and the reference signal stored within that radar [21], [22]. Therefore, the results in this article will apply to both QTMS radars and noise radars.

Apart from the fact that noise radars form a bridge between conventional radars and quantum radars, noise radars are attractive because they are inherently low-probability-of-intercept (LPI) radars [5]. Because they transmit only noise, they are unlikely to interfere with other devices because most devices are designed to cope with noise. This makes them suitable for settings, such as hospitals and airports, where interference must be avoided whenever possible. Moreover, QTMS radars in particular operate at very low signal powers, further enhancing its LPI properties. This also suits QTMS radars to biomedical sensing and imaging, where sensor powers are greatly limited for safety reasons [23], [24]. We wish to emphasize, however, that we do not advocate for the wholesale replacement of conventional radars. Noise radars and QTMS radars are merely additional tools in the toolbox.

In the case of noise radars and QTMS radars, it is typically assumed that the radar detection data are drawn from a multivariate normal distribution with zero mean [21], [25]. The question then becomes: what test statistic—or *detector function*—should the radar use when conducting the hypothesis test? Various detector functions have been proposed and analyzed in the past [22], [25], [26], but it appears that one particularly natural test statistic has hitherto escaped notice: the likelihood ratio (LR).

We now present an analysis of the detection performance of QTMS radars and noise radars when the LR is used for the derivation of detector functions. We explicitly derive an expression for a generalized likelihood ratio (GLR) detector function under certain simplifying assumptions. Although these assumptions mean that our analysis is not fully general, there nevertheless exist situations (especially in the biomedical realm) where such simplified assumptions are reasonable. We then derive an approximate GLR detector function which is appropriate when the radar attempts to detect a target that is small or far away. Theoretical expressions for the ROC curve are presented for the case of long radar integration times (large number of samples N), and simulation results are shown for short integration times (small number of samples). One major result of our work is that, because the Karlin–Rubin theorem [27] (a generalization of the Neyman–Pearson lemma) does not hold, the GLR detector is not necessarily optimal and there exists a parameter regime in which it is known to be outperformed by a detector function previously studied in [26]. Hence, the search for detector functions for QTMS radar and noise radar remains an open problem, although the GLR detector is a strong competitor.

This article builds on and greatly extends previous results which were submitted to two conferences [28], [29]. We have extended the work in [28] to include explicit expressions for the GLR detector and its ROC curve, compared the results to the approximations in [29], and included a small- N analysis which was missing from [29].

The rest of this article is organized as follows. Section II lays out the QTMS/noise radar detection problem in mathematical terms. We then derive an explicit expression for the GLR detector in Section III, together with an approximation thereto. We derive ROC curve expressions for the GLR detector in Section IV and confirm them with simulations. In Section V, we show that the GLR detector is not optimal under certain conditions, so it is not possible to make absolute statements about optimality. Section VI presents simulations of the behavior of the GLR detector when the number of samples integrated is small. Finally, Section VII concludes this article.

II. BACKGROUND

Noise radars and QTMS radars work by transmitting an electromagnetic noise signal toward a target, receiving the echo, and comparing the received signal with a reference signal stored within the radar. This is illustrated in Fig. 1. Every electromagnetic signal can be mathematically described by two real-valued time series, one representing the in-phase voltages of the signal and the other representing its quadrature voltages. In a noise radar, the two voltage time series of the transmitted signal are typically taken to be Gaussian white noise processes with zero mean, and all other noise sources inside and outside the radar are modeled as additive white Gaussian noise (AWGN). It follows that the voltage time series of the received signal are also Gaussian white noise. To our knowledge, all previous work on the theory of noise radar has made use of these assumptions. They are reasonable assumptions in practice, since it is not unreasonable to assume that the properties of the signal

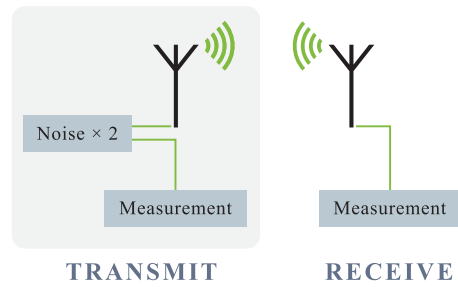


Fig. 1. Block diagram illustrating the basic idea of noise radar. This figure first appeared in [19].

generated by the radar are known, nor is it unreasonable to assume that external noise sources are AWGN unless this is specifically known to be false.

Let us denote the in-phase and quadrature voltages of the received signal by $I_1[n]$ and $Q_1[n]$, respectively, where n is the discrete time index. Similarly, let us denote the in-phase and quadrature voltages of the reference signal by $I_2[n]$ and $Q_2[n]$, respectively. As a consequence of the discussion above, each of these variables is a Gaussian white noise process with zero mean. They are “jointly white” in the sense that $I_1[n_0]$ and $I_2[n_1]$ are independent unless $n_0 = n_1$, and likewise for all other pairs of the four signals. Because this is so, we are only interested in the case where the time difference is zero, and we will suppress the variable n when no confusion arises.

It is evident that the four voltage signals are fully characterized by the 4×4 covariance matrix $E[\vec{x}\vec{x}^T]$, where $\vec{x} = [I_1, Q_1, I_2, Q_2]^T$. In [21], we showed that for a noise radar, $E[\vec{x}\vec{x}^T]$ can be written in block matrix form as

$$\Sigma = \begin{bmatrix} \sigma_1^2 \mathbf{1}_2 & \rho \sigma_1 \sigma_2 \mathbf{R}(\phi) \\ \rho \sigma_1 \sigma_2 \mathbf{R}(\phi)^T & \sigma_2^2 \mathbf{1}_2 \end{bmatrix} \quad (1)$$

where σ_1^2 and σ_2^2 are the received and reference signal powers, respectively, while ϕ is the phase shift between the signals, $\mathbf{1}_2$ is the 2×2 identity matrix, and $\mathbf{R}(\phi)$ is the rotation matrix

$$\mathbf{R}(\phi) = \begin{bmatrix} \cos \phi & \sin \phi \\ -\sin \phi & \cos \phi \end{bmatrix}. \quad (2)$$

QTMS radars are characterized by a similar matrix, but with a reflection matrix instead of a rotation matrix

$$\mathbf{R}'(\phi) = \begin{bmatrix} \cos \phi & \sin \phi \\ \sin \phi & -\cos \phi \end{bmatrix}. \quad (3)$$

For the purposes of this article, it is unimportant whether $\mathbf{R}(\phi)$ or $\mathbf{R}'(\phi)$ is used. The results will be the same in any case.

A. Target Detection Using the Correlation Coefficient

Out of the four parameters appearing in the covariance matrix (1), it is the correlation coefficient ρ , which is of greatest importance in the problem of target detection. When the target is absent, $\rho = 0$ because the received signal is purely background noise, which is completely independent of the radar’s internal reference signal. Conversely, when the target is present, $\rho > 0$ because some component of the received signal will have originated from the radar

and that component will be correlated with the reference signal. The detection problem for noise radar can, therefore, be formulated as the problem of distinguishing between the following hypotheses:

$$\begin{aligned} H_0 : \rho = 0 & \text{ Target absent} \\ H_1 : \rho > 0 & \text{ Target present.} \end{aligned} \quad (4)$$

At this point, we note that the “quantum advantage” of QTMS radars over standard noise radars lies in the fact that QTMS radars can achieve higher values of ρ [22]. This means that the two hypotheses are easier to distinguish, giving rise to an enhancement in detection performance.

In order to perform this hypothesis test, we must decide on a detector function (test statistic), which allows us to distinguish between the two cases. If we were working with only two time series, a natural choice would be to perform matched filtering. However, we are working with four time series, so we must find a detector that suitably generalizes the matched filter. Previous work has focused on a generalization of matched filtering to complex signals [25] or on estimating ρ directly [22]. In this article, we use a statistic based on the LR in order to derive a detector function.

There are, unfortunately, three other parameters to be accounted for: σ_1 , σ_2 , and ϕ . None of these play a direct role in distinguishing whether or not there is a target, and are hence “nuisance parameters.” The usual methods for dealing with nuisance parameters (e.g., integrating them out) appear to yield complicated and intractable expressions. Therefore, in the derivation of the GLR detector, we make the simplifying assumptions $\sigma_1 = \sigma_2 = 1$ and $\phi = 0$. This amounts to a normalization and standardization of the radar’s detection data. The time series are normalized to have variance 1, while the reference signal in the radar is “rotated” so that there is no phase shift between it and the received signal.

These assumptions are admittedly rather restrictive. However, we will show in Section IV-A that our results hold even when $\sigma_1 = \sigma_2 = 1$ is violated, so this assumption really only serves to simplify the derivations and does not substantively affect our results. This leaves the $\phi = 0$ assumption. Unlike the $\sigma_1 = \sigma_2 = 1$ assumption, violation of the $\phi = 0$ assumption does in fact lead to a decrease in detection performance. The tradeoff is that, phase-sensitive detectors tend to outperform phase-insensitive detectors. Thus, our work gives us some idea of the best performance that can be obtained from a noise radar or QTMS radar. Moreover, in the case of a stationary target, an artificial phase shift can be injected into the reference signal to maximize the detection performance: all that is needed is to apply an appropriate rotation matrix to I_2 and Q_2 . This is a 1-D maximization over a very limited search space, which is easy to perform. One application where stationarity can be justified is biomedical sensing, one of the most promising applications for QTMS radar [24]. Typically, the distance from a sensor to a patient is fixed, so the phase is not expected to change significantly. For the more general case of slowly-varying ϕ , the artificial phase shift could even be adjusted using adaptive signal-processing techniques. We point out, too, that the $\phi = 0$ assumption was made in

previous theoretical and experimental work [19], [26], [30], so the results given can be directly compared with previous research.

B. QTMS/Noise Radar Detection Problem

With the above discussion in mind, we may formulate the QTMS/noise radar detection problem as follows: let N independent samples be drawn from a multivariate normal distribution with zero mean and covariance matrix

$$\Sigma(\rho) = \begin{bmatrix} 1 & 0 & \rho & 0 \\ 0 & 1 & 0 & \pm\rho \\ \rho & 0 & 1 & 0 \\ 0 & \pm\rho & 0 & 1 \end{bmatrix} \quad (5)$$

where the positive sign should be used for noise radars and the negative sign for QTMS radars. (Note that N is related to the integration time T and the sampling frequency f_s of the radar by $T = N/f_s$.) Given these samples, we must decide whether $\rho = 0$ or $\rho > 0$. Our approach will be to use the LR to distinguish between these two hypotheses.

In the calculations that follow, we will assume the use of a QTMS radar and use the negative sign in (5). To apply our results to standard noise radars, only one sign change is necessary, as we will indicate below.

C. Simulation Procedure

In this article, we will have recourse to computer simulations to supplement our theoretical calculations. Naively, we would simply generate N random vectors every time we wish to simulate a single value of the detector function. However, we will see that the LR depends on the data only through the sample covariance matrix

$$\tilde{\mathbf{S}} = \frac{1}{N} \sum_{n=1}^N \vec{x}_n \vec{x}_n^T \quad (6)$$

where \vec{x}_n is the n th sample vector. It is unnecessary, therefore, to generate N random vectors. We need only draw a single random matrix from the Wishart distribution $W_4(\mathbf{\Sigma}, N)$, then normalize the result by N . This was the procedure used in [22]; it leads to significantly shorter computation times.

In all cases where we obtain ROC curves by simulation, we generate 10^7 random matrices with $\rho = 0$ and another 10^7 with a given value of $\rho > 0$. These correspond to the cases where the radar target is absent or present, respectively. From these matrices, we calculate 10^7 simulated detector function outputs for each case. The ROC curves are, then, obtained by using the histograms of detector function outputs as empirical probability density functions.

III. GLR DETECTOR

As mentioned previously, one way to test between the hypotheses in (4) is to perform an LR test. We now derive an explicit expression for the GLR detector function.

The probability density function for a k -dimensional multivariate normal distribution with mean vector $\vec{\mu}$ and covariance matrix $\mathbf{\Sigma}$ is

$$f(x) = \frac{\exp\left[-\frac{1}{2}(\vec{x} - \vec{\mu})^T \mathbf{\Sigma}^{-1}(\vec{x} - \vec{\mu})\right]}{\sqrt{(2\pi)^k |\mathbf{\Sigma}|}} \quad (7)$$

where $|\Sigma|$ is the determinant of Σ . It follows immediately that, for N independently drawn samples $\vec{x}_1, \dots, \vec{x}_N$, the log-likelihood is

$$\ell(\vec{\mu}, \Sigma) = -\frac{N}{2}[\ln |\Sigma| + k \ln(2\pi)] - \frac{1}{2} \sum_{i=1}^N (\vec{x}_i - \vec{\mu})^T \Sigma^{-1} (\vec{x}_i - \vec{\mu}). \quad (8)$$

Substituting (5) along with $k = 4$ and $\vec{\mu} = [0, 0, 0, 0]^T$, we find that the log-likelihood function for QTMS radar is

$$\ell(\rho) = -\frac{N}{2} \left[\frac{\bar{P}_{\text{tot}} - 2\bar{D}_1\rho}{1 - \rho^2} + 2 \ln(1 - \rho^2) + 4 \ln(2\pi) \right] \quad (9)$$

where, for brevity, we define

$$P_{\text{tot}} \equiv I_1^2 + Q_1^2 + I_2^2 + Q_2^2 \quad (10)$$

$$D_1 \equiv I_1 I_2 - Q_1 Q_2. \quad (11)$$

In (9) and elsewhere in this article, a line over an expression indicates the sample mean. For example

$$\overline{I_1 I_2} = \frac{1}{N} \sum_{n=1}^N i_1^{(n)} i_2^{(n)} \quad (12)$$

where $i_1^{(n)}$ and $i_2^{(n)}$ denote the n th samples of I_1 and I_2 , respectively.

As mentioned previously, we have taken the negative sign in (5). The only change needed when the positive sign is used is to set $D_1 \equiv I_1 I_2 + Q_1 Q_2$.

We can interpret P_{tot} as the total power at the radar receiver; it is the sum of the powers of the in-phase and quadrature components of both the received signal and the reference signal. The quantity D_1 appeared in [19] under the name ‘‘Detector 1’’ and was studied in further depth in a previous publication [26].

Having written down the log-likelihood, we can now define the GLR detector.

DEFINITION The *GLR detector* is defined as

$$D_{\text{GLR}} = -2[\ell(0) - \ell(\hat{\rho})] = N \left[\frac{2\bar{D}_1 \hat{\rho} - \bar{P}_{\text{tot}} \hat{\rho}^2}{1 - \hat{\rho}^2} - 2 \ln(1 - \hat{\rho}^2) \right] \quad (13)$$

where $\hat{\rho}$ is the maximum likelihood estimate of ρ .

REMARK The factor of -2 ensures compatibility with Wilks’ theorem, which we will invoke in the following section.

PROPOSITION 1 The maximum likelihood estimate of ρ is

$$\hat{\rho} = \frac{1}{6} \left(w - \frac{A_1}{w} + \bar{D}_1 \right) \quad (14)$$

where

$$A_1 = 6(\bar{P}_{\text{tot}} - 2) - \bar{D}_1^2 \quad (15a)$$

$$A_2 = (72 - 9\bar{P}_{\text{tot}} + \bar{D}_1^2)\bar{D}_1 \quad (15b)$$

$$w = \sqrt[3]{A_2 + \sqrt{A_1^3 + A_2^2}}. \quad (15c)$$

In (15c), we must choose the appropriate cube and square roots to ensure that $0 < \hat{\rho} < 1$.

PROOF In order to obtain the maximum likelihood estimate $\hat{\rho}$, we must maximize the log-likelihood (9). To this end, we calculate the derivative of $\ell(\rho)$ as follows:

$$\frac{d\ell(\rho)}{d\rho} = N \frac{\bar{D}_1 - (\bar{P}_{\text{tot}} - 2)\rho + \bar{D}_1\rho^2 - 2\rho^3}{(1 - \rho^2)^2}. \quad (16)$$

Assuming that $0 < \hat{\rho} < 1$, the maximum likelihood estimate will occur when $d\ell(\rho)/d\rho = 0$. This is equivalent to solving the cubic equation

$$\bar{D}_1 - (\bar{P}_{\text{tot}} - 2)\rho + \bar{D}_1\rho^2 - 2\rho^3 = 0. \quad (17)$$

The general form for the solution of a cubic equation is known, so the proposition immediately follows. ■

A. Approximate GLR Detector

Because the GLR detector is unwieldy, we shall derive an approximate form of the detector function. In order to do so, we will assume that $\rho \ll 1$. This regime is of great importance for radar detection because it corresponds to targets that are difficult to detect. For example, they may be far away from the radar, or they could have very small radar cross sections, or the signal-to-noise ratio may be unfavorable. All these cases would lead to a small correlation coefficient [31]. Therefore, the assumption $\rho \ll 1$ is not merely a mathematical convenience; this assumption has practical significance.

The following proposition gives a second-order approximation of the GLR detector. This approximation is much easier to calculate than the exact GLR detector and is more numerically stable, an important consideration when processing power is limited.

PROPOSITION 2 The GLR detector may be approximated by the following formula, which is correct up to second order in ρ :

$$D_{\text{GLR}} \approx \frac{N\bar{D}_1^2}{\bar{P}_{\text{tot}} - 2}. \quad (18)$$

PROOF Under the small- ρ assumption, we may expand (13) around $\hat{\rho} = 0$ in powers of $\hat{\rho}$, keeping terms up to second order. The result is

$$D_{\text{GLR}} \approx N\hat{\rho}[2\bar{D}_1 - (\bar{P}_{\text{tot}} - 2)\hat{\rho}]. \quad (19)$$

Since ρ is small, we may obtain an approximation of $\hat{\rho}$ by keeping terms up to first order in (17) (which is equivalent to keeping terms up to second order in the log-likelihood itself). The resulting equation is linear, and its solution is

$$\hat{\rho} \approx \frac{\bar{D}_1}{\bar{P}_{\text{tot}} - 2}. \quad (20)$$

By substituting this into (19), we obtain (18).

REMARK It is of interest to note that the approximate GLR detector function (18) can be obtained directly from the exact expressions (13) and (14) by expanding in powers of \bar{D}_1 and retaining the lowest order term. (This can be verified using a computer algebra system, such as Mathematica.) The two approaches are roughly equivalent because

$E[D_1] = 2\rho$, so when ρ is small, \bar{D}_1 may be expected to be small as well.

IV. ROC CURVE FOR THE GLR DETECTOR

It follows from Wilks' theorem that, under H_0 (target absent), the distribution of the detector in the limit $N \rightarrow \infty$ is $D_{\text{GLR}} \sim \chi_1^2$, a chi-square distribution with one degree of freedom [32]. The fact that there is one degree of freedom follows from the fact that ρ is a 1-D quantity and that the parameter space under H_0 is zero-dimensional, being the single point $\rho = 0$.

An approximation to the distribution of D_{GLR} under H_1 (target present) can be obtained by appealing to [33, Th. 1]. That theorem is extremely general and we are only interested in the specific case where the likelihood function contains only one parameter to test and no nuisance parameters. In the following lemma, we restate the theorem for the specific case we are interested in.

LEMMA 1 Let N samples be drawn from a family of probability distributions parameterized by θ , let δ be a constant, and let λ_N be the LR for testing the following hypotheses:

$$\begin{aligned} H_0 : \theta &= \theta_0 \\ H_1 : \theta &= \theta_0 + \frac{\delta}{\sqrt{N}}. \end{aligned} \quad (21)$$

Finally, let $\mathcal{I}(\theta)$ be the Fisher information for the family of distributions from which the samples were drawn. Then, under the alternative hypothesis H_1 , it is true that

$$-2 \ln \lambda_N \xrightarrow{d} \chi_1^2[\delta^2 \mathcal{I}(\theta_0)]. \quad (22)$$

In other words, as $N \rightarrow \infty$, the statistic $-2 \ln \lambda_N$ converges in distribution to the noncentral chi-square distribution with one degree of freedom and noncentrality parameter $\delta^2 \mathcal{I}(\theta_0)$.

PROOF This is a special case of [33, Th. 1]. ■

Note that by taking $\delta = 0$, we immediately recover Wilks' theorem as a special case.

We now use this lemma to determine the distribution of the GLR detector.

PROPOSITION 3 In the limit $N \rightarrow \infty$,

$$D_{\text{GLR}} \sim \chi_1^2(2N\rho^2). \quad (23)$$

PROOF In Lemma 1, substitute $\theta = \rho$, $\theta_0 = 0$, and $\delta = \rho\sqrt{N}$. (Technically, this is not fully legitimate because δ should not depend on N . However, we will show via simulations that for small ρ , we still obtain a satisfactory result.) We also need the Fisher information

$$\begin{aligned} \mathcal{I}(\rho) &= -E \left[\frac{\partial^2}{\partial \rho^2} \ell(\rho) \right] \\ &= E \left[\frac{-2 + P_{\text{tot}}(1 + 3\rho^2) - 2D_1\rho(3 + \rho^2) + 2\rho^4}{(1 - \rho^2)^3} \right] \\ &= \frac{1}{(1 - \rho)^2} + \frac{1}{(1 + \rho)^2}. \end{aligned} \quad (24)$$

The final line was obtained by using the linearity of the expectation value operator, inspecting the definitions of P_{tot} and D_1 in (10) and (11), respectively, then reading off the

appropriate entries of (1). Note that in calculating the Fisher information, we must take $N = 1$ in $\ell(\rho)$.

Once we make the appropriate substitutions in (22), the proposition follows immediately. ■

When ρ is small and the second-order approximation (18) applies, we can give an alternate plausibility argument for Proposition 3. This argument requires only elementary statistics and is perhaps more insightful than the abovementioned proof.

First, note that under the central limit theorem \bar{D}_1 is normally distributed with mean 2ρ and variance $2(1 + \rho^2)/N$ when N is large [26]. Since (18) holds when $\rho \ll 1$, we may simplify this and state that $\bar{D}_1 \sim \mathcal{N}(2\rho, 2/N)$. Let us introduce the transformed random variable

$$X \equiv \sqrt{\frac{N}{2}} \bar{D}_1. \quad (25)$$

It follows from the properties of the normal distribution that $X \sim \mathcal{N}(\rho\sqrt{2N}, 1)$.

We now argue that $\bar{P}_{\text{tot}} \sim \mathcal{N}(4, 8/N)$. It is easy to see that $E[P_{\text{tot}}] = 4$; this follows directly from (5) and (10). The calculation of $\text{var}[P_{\text{tot}}]$ is more difficult because it involves terms of the form $\text{cov}[I_1^2, I_2^2]$. Luckily, a result in [34] allows us to calculate such expressions. A special case of this result is quoted in the following lemma.

LEMMA 2 Let x, y, u , and v be jointly normal random variables, each with zero mean. Then

$$\text{cov}[xy, uv] = \text{cov}[x, u] \text{cov}[y, v] + \text{cov}[x, v] \text{cov}[y, u]. \quad (26)$$

PROOF This is a special case of [34, eq. (13)].

By applying this lemma repeatedly, we find that $\text{var}[P_{\text{tot}}] = 8(1 + \rho^2)$, which can be simplified to $\text{var}[P_{\text{tot}}] = 8$ because ρ is assumed to be small. Since N is large, we again invoke the central limit theorem to state that $\bar{P}_{\text{tot}} \sim \mathcal{N}(4, 8/N)$.

Let us define

$$Y \equiv \frac{\bar{P}_{\text{tot}}}{2} - 1. \quad (27)$$

From the properties of the normal distribution, $Y \sim \mathcal{N}(1, 2/N)$. Moreover

$$D_{\text{GLR}} \approx \frac{N\bar{D}_1^2}{\bar{P}_{\text{tot}} - 2} = \frac{X^2}{Y}. \quad (28)$$

As $N \rightarrow \infty$, the variance of Y approaches zero and Y converges in probability to 1. Therefore, $D_{\text{GLR}} \approx X^2$. But X^2 is the square of a normally distributed random variable with variance 1, so it is a noncentral chi-square random variable with one degree of freedom and noncentrality parameter $(\rho\sqrt{2N})^2$. Once again, Proposition 3 follows.

Now that we know the distribution of D_{GLR} conditioned on whether the target is present or absent, we can easily derive an expression for the ROC curve of the GLR detector.

PROPOSITION 4 In the limit $N \rightarrow \infty$, the ROC curve for the GLR detector is

$$p_D(p_{\text{FA}}) = Q_{\frac{1}{2}} \left[\rho\sqrt{2N}, \sqrt{S^{-1}(p_{\text{FA}})} \right] \quad (29)$$

where $Q_{1/2}$ denotes the Marcum Q-function of order 1/2, S^{-1} is the inverse of the function defined as

$$S(T) \equiv 1 - P\left(\frac{1}{2}, \frac{T}{2}\right) \quad (30)$$

and P is the regularized gamma function.

PROOF If the target is absent, $D_{\text{GLR}} \sim \chi_1^2$ in the limit $N \rightarrow \infty$ by Wilks' theorem. The cumulative density function for the χ_1^2 distribution is known to be $P(1/2, x/2)$, whose survival function is $S(T)$. Therefore, the probability of false alarm for a given threshold T is $p_{fa} = S(T)$.

If the target is present, we know from Proposition 3 that $D_{\text{GLR}} \sim \chi_1^2(2N\rho^2)$ as $N \rightarrow \infty$. The survival function for the $\chi_1^2(2N\rho^2)$ distribution is $Q_{1/2}(\rho\sqrt{2N}, \sqrt{T})$. The proposition follows upon substituting $T = S^{-1}(p_{fa})$. ■

REMARK As noted in Section II-A, we assumed that the phase ϕ between the received and reference signals in the radar was equal to zero. The effect of loosening this assumption can be seen by observing that the GLR detector depends on the measurement data only through P_{tot} (10) and D_1 (11). Of these, P_{tot} is phase-invariant, while $E[D_1]$ is proportional to $\rho \cos \phi$. It follows that the ROC curve for the GLR detector when $\phi \neq 0$ is the same as in (29), but with ρ replaced by $\rho \cos \phi$. This suggests that one method of estimating ϕ (when sufficient data and time are available) is to apply a rotation matrix to the I and Q voltages of the reference signal to artificially induce a phase shift, then find the rotation angle that maximizes the ROC curve. One simplistic way to do this is with a battery of GLR detectors, each at a different phase shift; the number of detectors need not be very large.

As for the $\sigma_1 = \sigma_2 = 1$ assumption, we will show in the following section that this assumption is not strictly needed for (29) to hold.

A. Simulations

In order to bolster our confidence in the ROC curve formula (29) and the small- ρ approximation (18), we verified these expressions using simulations as described in Section II-C. This is desirable because Lemma 1 was not strictly satisfied when we invoked it to prove Proposition 3. In Fig. 2, we can see that the resulting histograms match up with the theoretical distributions obtained above. In Fig. 3, we plotted the ROC curves that arise from the simulations. The results show that the simulated data agrees extremely closely with the theoretical expression (29), at least for small values of ρ .

In Fig. 4, we show how p_d behaves as a function of ρ for various fixed values of p_{fa} . This plot corresponds to the plots of p_d versus single-pulse SNR that are often seen in the radar literature, except that ρ takes the place of SNR and Fig. 4 is not for the single-pulse case (we have used $N = 50\,000$).

We will now show that, although the approximate GLR detector was derived under the assumption that $\sigma_1 = \sigma_2 = 1$ in (1), it is nevertheless still a viable detector function when σ_1 and σ_2 are unknown. In Fig. 5, we plot simulated ROC curves for the approximate GLR detector when $(\sigma_1, \sigma_2) = (0.1, 10)$ and $(0.01, 10\,000)$. Even in the

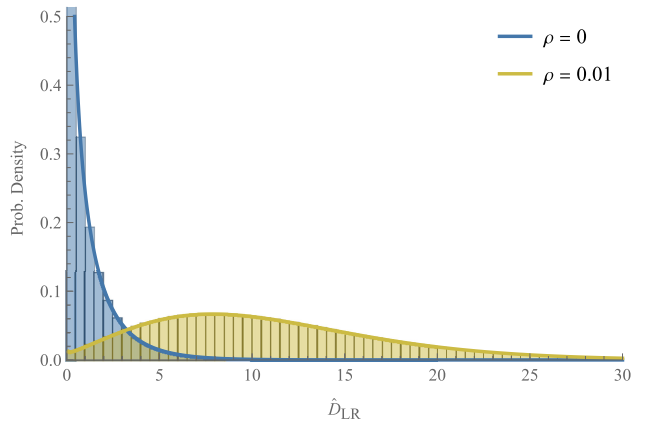


Fig. 2. Histograms of simulated GLR detector outputs for $N = 50\,000$, plotted together with theoretical probability density functions. Blue: $\rho = 0$. Orange: $\rho = 0.01$.

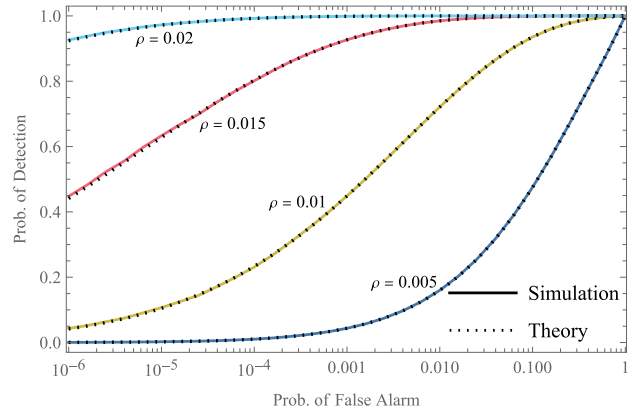


Fig. 3. Comparison of simulated ROC curves for the GLR detector with theoretical ROC curves calculated from (29) for $N = 50\,000$ and varying values of ρ .

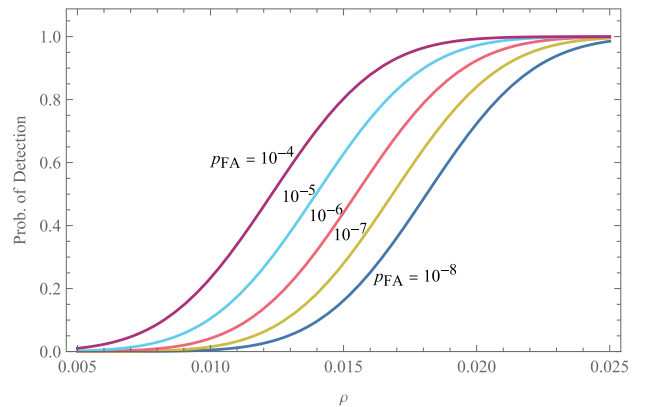
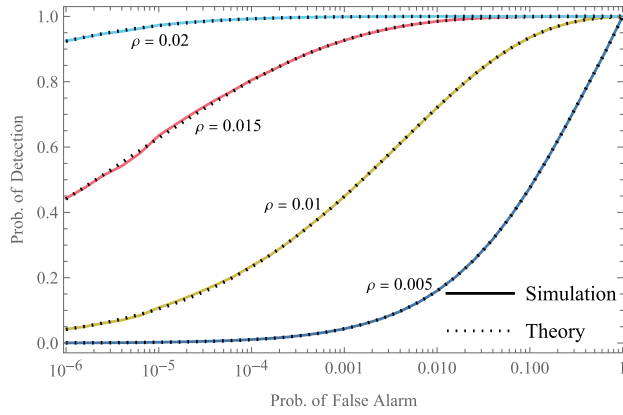
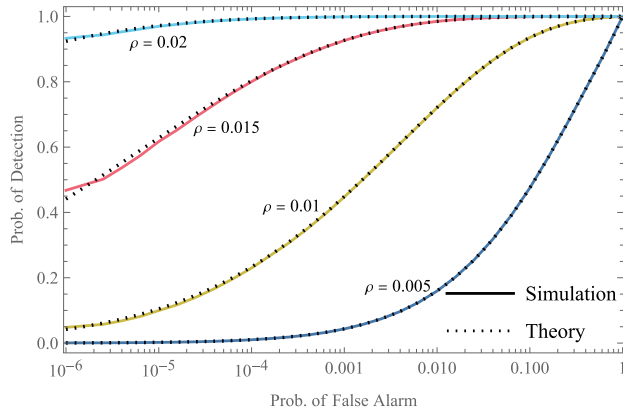


Fig. 4. Probability of detection p_d as a function of ρ for the GLR detector for various values of p_{fa} , calculated from (29) with $N = 50\,000$.

second case, where there is a large deviation from the assumption $\sigma_1 = \sigma_2 = 1$, the ROC curves do not noticeably deviate from the theoretical expression (29). From these results, it appears plausible that so long as $\rho \ll 1$ and $\bar{P}_{\text{tot}} > 2$, the approximate GLR detector gives results that are reasonably close to the theoretical expression (29). [The condition $\bar{P}_{\text{tot}} > 2$ is necessary because, otherwise, the



(a)



(b)

Fig. 5. Comparison of simulated and theoretical ROC curves for the approximate GLR detector when (σ_1, σ_2) equals (a) $(0.1, 10)$ and (b) $(0.01, 10000)$. In all cases, $N = 50000$.

denominator of (18) would become negative, but this can trivially be achieved by multiplying all I and Q voltages by a sufficiently large scaling factor.]

Although Fig. 5 shows plots for the approximate GLR detector, simulations using the exact GLR detector show the same behavior, so the assumption $\sigma_1 = \sigma_2 = 1$ is unnecessary for either version of the detector. Recall that only the approximate detector requires $\rho \ll 1$. Therefore, we may state that the exact GLR detector is viable even if the powers of the radar signals are unknown, irrespective of whether $\rho \ll 1$ holds or not.

V. NONOPTIMALITY OF THE GLR DETECTOR

It is well known that, according to the Neyman–Pearson lemma, the (nongeneralized) LR test is the most powerful one when deciding between two simple hypotheses [27]. Referring back to (4), however, we see that the target detection problem does not satisfy the premises of the Neyman–Pearson lemma. The hypothesis that a target is present is not a simple hypothesis. We are not deciding between $\rho = 0$ and $\rho = \rho_0$ for some known value ρ_0 . It is, therefore, not permissible to rely on the Neyman–Pearson lemma to state that the LR test is optimal.

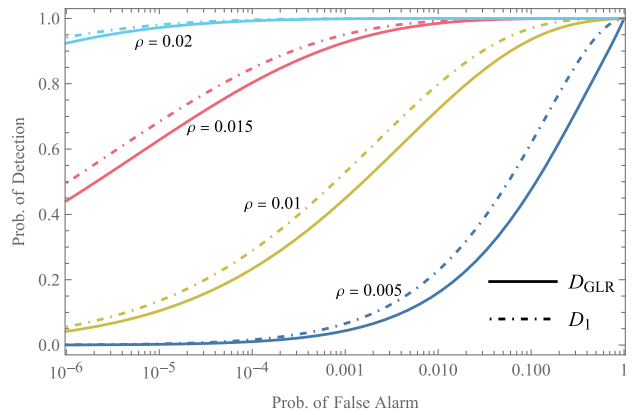


Fig. 6. Comparison of the GLR detector with D_1 for $N = 50000$ and various values of ρ .

There is, however, an extension to the Neyman–Pearson lemma which applies to composite hypotheses of the type seen in (4): the Karlin–Rubin theorem [27]. It states that the LR test is the most powerful test for one-sided composite hypotheses, such as (4), when certain conditions are satisfied. One of these conditions is that there exist a scalar-valued sufficient statistic $T(x)$ for ρ . The Fisher–Neyman factorization theorem states that $T(x)$ is a sufficient statistic for ρ if and only if the LR factorizes into the form $h(x)g_\rho[T(x)]$, where $h(x)$ does not depend on ρ while $g_\rho[T(x)]$ depends on the data x only through the statistic $T(x)$. Such a statistic T , however, cannot be found. To see this, it is necessary only to inspect the log-likelihood (9). It is clear that $g_\rho[T(x)]$ satisfies

$$\ln g_\rho[T(x)] = -\frac{N}{2} \left[\frac{\bar{P}_{\text{tot}} - 2\bar{D}_1\rho}{1 - \rho^2} + 2 \ln(1 - \rho^2) \right]. \quad (31)$$

But this expression depends on the data through *two* statistics, namely \bar{P} and \bar{D}_1 . There is no way to combine \bar{P} and \bar{D}_1 so that (32) is a function of a single scalar-valued statistic for ρ . Therefore, the LR does not factor into the form $h(x)g_\rho[T(x)]$ when T is a scalar, and there exists no scalar-valued sufficiently statistic. It follows that the Karlin–Rubin theorem does not apply, and we cannot rely on this theorem to state that the LR test is optimal.

The above discussion shows that the GLR detector is not necessarily the most powerful detector for the target detection problem. It serves as a plausibility argument for the following proposition, which would otherwise appear surprising.

PROPOSITION 5 The GLR detector is not optimal.

PROOF Fig. 6 shows the ROC curves that would be obtained when D_1 is used as a detector function. There is a small but clear advantage in using D_1 for target detection compared to using D_{GLR} , at least for certain values of ρ and N . Therefore, the GLR detector is not optimal. ■

In the discussion following the definition of D_1 in (11), we noted that the use of D_1 as a detector function was studied in [19]. When $\sigma_1 = \sigma_2 = 1$, $\phi = 0$, and $N \rightarrow \infty$, the ROC

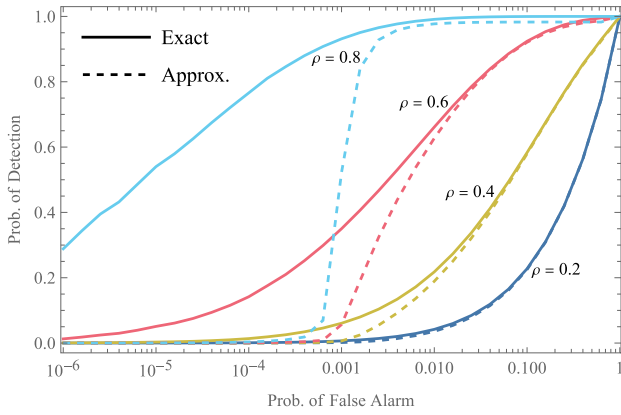


Fig. 7. Comparison of simulated ROC curves for the exact GLR detector (13) with the small- ρ approximation (18) for $N = 10$ and various values of ρ .

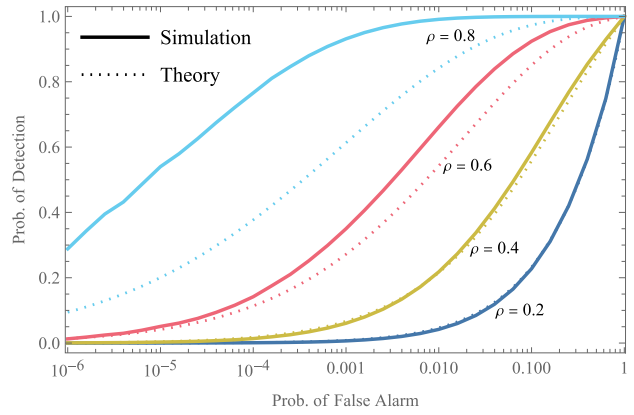


Fig. 8. Comparison of simulated ROC curves for the GLR detector with theoretical ROC curves calculated from (29) for $N = 10$ and various values of ρ .

curve for D_1 is

$$p_d(p_{fa}) = \frac{1}{2} \operatorname{erfc} \left(\frac{\operatorname{erfc}^{-1}(2p_{fa}) - \sqrt{N}\rho}{\sqrt{1 + \rho^2}} \right) \quad (32)$$

where erfc is the complementary error function. These parameter values were chosen in order to obtain an expression that can be compared with (29), which was derived assuming the same parameter values.

We do not claim that D_1 outperforms D_{GLR} in all cases. On the contrary, we will show in the following section that when N is small, there are regimes where the GLR detector is better than D_1 . Therefore, it is not possible to make blanket statements about the superiority of one detector over another, and the search for good detector functions remains an open problem.

VI. SIMULATION RESULTS FOR SMALL N

The ROC curve expressions in the previous section have all been derived under the assumption that the number of samples N is large. However, in the context of radar detection, it is not always possible to use very large values of N . This corresponds to the use of long integration times, which is undesirable in situations where radars need to detect targets quickly. Therefore, it is of interest to characterize the detection performance of the GLR detector for small N . Unfortunately, there are no analytical results that we can rely upon. We, therefore, turn to simulations.

We note that, when N is small, it is necessary that ρ be made larger in order to compensate. For this reason, the results in this section apply to cases where the target is easier to detect (e.g., smaller range or larger radar cross section) and we wish to detect the target very quickly.

Our first comparison is between the GLR detector (13) and the approximate detector (18). We have shown previously that, even if the assumption that $\sigma_1 = \sigma_2 = 1$ is violated, the approximate detector is still viable. If we could show that it is similarly viable when the assumption $\rho \ll 1$ is violated, we could eschew the use of the exact GLR detector (13) altogether. This would be desirable because the approximate detector requires far less computational

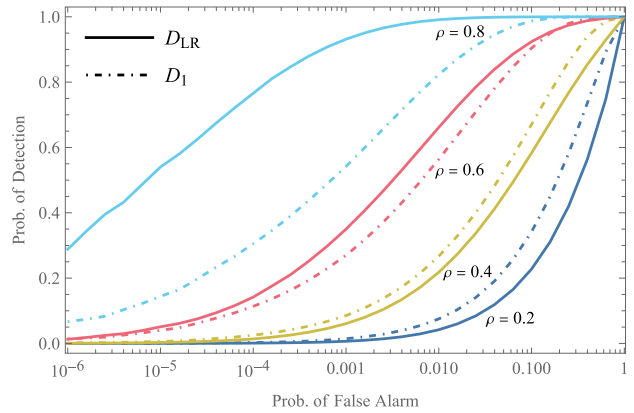


Fig. 9. Simulated ROC curves for the GLR detector compared with the D_1 detector for $N = 10$ and various values of ρ .

requirements. Unfortunately, as shown in Fig. 7, the approximate GLR detector does not perform nearly as well as the exact GLR detector when ρ is high.

Our next comparison is between simulated ROC curves for the exact GLR detector and the corresponding theoretical ROC curves calculated using (29). The motivation is to see how far we may rely on the theoretical expression even when ρ is large and N is small. Fig. 8 shows that, in fact, (29) is not reliable for large ρ and small N . As a matter of fact, when ρ is very large, the simulated ROC curves are significantly better than the corresponding theoretical ROC curves.

Finally, we compare the performance of the (exact) GLR detector with the D_1 detector function. As we already saw in Fig. 6, the theoretical ROC curve expressions show that D_1 is a better detector function when ρ is small. However, the simulation results in Fig. 9 suggest that there is a crossover in detection performance, and when ρ is high, D_{GLR} is better than D_1 . Therefore, we are not justified in making blanket statements about the optimality of any detector function. Instead, it may be a better strategy to choose D_{GLR} when ρ is expected to be large, and D_1 when ρ is expected to be small.

VII. CONCLUSION

In this article, we derived and analyzed two detector functions for QTMS radar and noise radar that are based on the LR. In addition to an exact formula for the GLR detector, we derived an approximate detector function that holds in the limit of small correlation coefficients ρ . We derived a mathematical formula for the ROC curve of the GLR detector which holds when the number of samples N is large; we also performed simulations to understand the behavior of the detector when N is small. We found that the GLR detector is not optimal, which runs counter to the intuition that the LR test is optimal or nearly so; it is outperformed by the D_1 detector function when ρ is small. However, the GLR detector is a strong competitor, significantly outperforming D_1 when ρ is very large and N is small.

One drawback of our work is that it assumes that the values of the nuisance parameters σ_1 , σ_2 , and ϕ are known. Although there exist situations where this is a reasonable assumption, especially in the context of biomedical sensing, it would be more satisfying if we could derive the GLR detector function without the use of these assumptions. This will be the subject of future work.

ACKNOWLEDGMENT

The authors would like to thank Dr. I. W. K. Lam for valuable discussions and for bringing [33] to our attention.

REFERENCES

- [1] C. W. Helstrom
Elements of Signal Detection and Estimation. Hoboken, NJ, USA: Prentice-Hall, 1995.
- [2] G. R. Cooper *et al.*
Random signal radar
Purdue Univ., Lafayette, IN, USA, Tech. Rep. TR-EE 67-11, Jun. 1967.
- [3] K. A. Lukin
Millimeter wave noise radar technology
In *Proc. 3rd Int. Kharkiv Symp. Phys. Eng. Microw., Millimeter Submillimeter Waves*, 1998, pp. 94-97.
- [4] Y. Zhang and R. M. Narayanan
Design considerations for a real-time random-noise tracking radar
IEEE Trans. Aerosp. Electron. Syst., vol. 40, no. 2, pp. 434-445, Apr. 2004.
- [5] T. Thayaparan and C. Wernik
Noise radar technology basics
Defence Res. Develop. Canada, *Tech. Mem. DRDC Ottawa TM 2006-266*, Dec. 2006.
- [6] K. A. Lukin *et al.*
Ka-band bistatic ground-based noise waveform SAR for short-range applications
IET Radar, Sonar Navig., vol. 2, no. 4, pp. 233-243, Aug. 2008.
- [7] D. Tarchi, K. Lukin, J. Fortuny-Guasch, A. Mogyla, P. Vyplavin, and A. Sieber
SAR imaging with noise radar
IEEE Trans. Aerosp. Electron. Syst., vol. 46, no. 3, pp. 1214-1225, Jul. 2010.
- [8] K. Kulpa
Signal Processing in Noise Waveform Radar. Norwood, MA, USA: Artech House, 2013.
- [9] R. Narayanan
Noise radar techniques and progress
In *Advanced Ultrawideband Radar: Signals, Targets, and Applications*, J. D. Taylor, Ed. Boca Raton, FL, USA: CRC Press, 2016, pp. 323-361.
- [10] K. Savci *et al.*
Trials of a noise-modulated radar demonstrator—first results in a marine environment
In *Proc. 20th Int. Radar Symp.*, 2019, pp. 1-9.
- [11] C. Wasserzier, J. G. Worms, and D. W. O'Hagan
How noise radar technology brings together active sensing and modern electronic warfare techniques in a combined sensor concept
In *Proc. Sensor Signal Process. Defence Conf.*, 2019, pp. 1-5.
- [12] K. Savci *et al.*
Noise radar—Overview and recent developments
IEEE Aerosp. Electron. Syst. Mag., vol. 35, no. 9, pp. 8-20, Sep. 2020.
- [13] S. Lloyd
Enhanced sensitivity of photodetection via quantum illumination
Science, vol. 321, no. 5895, pp. 1463-1465, Sep. 2008.
- [14] S.-H. Tan *et al.*
Quantum illumination with Gaussian states
Phys. Rev. Lett., vol. 101, Dec. 2008, Art. no. 253601.
- [15] E. D. Lopaeva, I. R. Berchera, I. P. Degiovanni, S. Olivares, G. Brida, and M. Genovese
Experimental realization of quantum illumination
Phys. Rev. Lett., vol. 110, Apr. 2013, Art. no. 153603.
- [16] B. Balaji and D. England
Quantum illumination: A laboratory investigation
In *Proc. Int. Carnahan Conf. Secur. Technol.*, 2018, pp. 1-4.
- [17] C. W. S. Chang, A. M. Vadiraj, J. Bourassa, B. Balaji, and C. M. Wilson
Quantum-enhanced noise radar
Appl. Phys. Lett., vol. 114, no. 11, Mar. 2019, Art. no. 112601.
- [18] D. Luong, A. Damini, B. Balaji, C. W. S. Chang, A. M. Vadiraj, and C. Wilson
A quantum-enhanced radar prototype
in *Proc. IEEE Radar Conf.*, 2019, pp. 1-6.
- [19] D. Luong, C. W. S. Chang, A. M. Vadiraj, A. Damini, C. M. Wilson, and B. Balaji
Receiver operating characteristics for a prototype quantum two-mode squeezing radar
IEEE Trans. Aerosp. Electron. Syst., vol. 56, no. 3, pp. 2041-2060, Jun. 2020.
- [20] D. Luong, S. Rajan, and B. Balaji
Entanglement-based quantum radar: From myth to reality
IEEE Aerosp. Electron. Syst. Mag., vol. 35, no. 4, pp. 22-35, Apr. 2020.
- [21] D. Luong and B. Balaji
Quantum two-mode squeezing radar and noise radar: Covariance matrices for signal processing
IET Radar, Sonar Navig., vol. 14, no. 1, pp. 97-104, Jan. 2020.
- [22] D. Luong, S. Rajan, and B. Balaji
Quantum two-mode squeezing radar and noise radar: Correlation coefficients for target detection
IEEE Sensors J., vol. 20, no. 10, pp. 5221-5228, May 2020.
- [23] S. Pisa, E. Pittella, and E. Piuizi
A survey of radar systems for medical applications
IEEE Aerosp. Electron. Syst. Mag., vol. 31, no. 11, pp. 64-81, Nov. 2016.
- [24] D. Luong, S. Rajan, and B. Balaji
Biomedical sensing using quantum radars based on Josephson parametric amplifiers
In *Proc. Int. Appl. Comput. Electromagn. Soc. Symp.*, 2021, pp. 1-4.

- [25] M. Dawood and R. M. Narayanan
Receiver operating characteristics for the coherent UWB random noise radar
IEEE Trans. Aerosp. Electron. Syst., vol. 37, no. 2, pp. 586–594, Apr. 2001.
- [26] D. Luong, B. Balaji, and S. Rajan
Simulation study of a detector function for QTMS radar and noise radar
in *Proc. IEEE Radar Conf.*, 2020, pp. 1–5.
- [27] G. Casella and R. L. Berger
Statistical Inference, 2nd ed. Duxbury, MA, USA: Brooks/Cole Cengage Learn, 2002.
- [28] D. Luong, B. Balaji, and S. Rajan
When should we use likelihood ratio target detection with QTMS radar and noise radar?
in *Proc. 2021 IEEE Radar Conf.*, 2021, pp. 1–5.
- [29] D. Luong, B. Balaji, and S. Rajan
An approximate likelihood ratio detector for QTMS radar and noise radar
In *Proc. Int. Conf. Sensor Signal Process. Defence*, 2021, pp. 1–5.
- [30] S. Barzanjeh, S. Pirandola, D. Vitali, and J. M. Fink
Microwave quantum illumination using a digital receiver
Sci. Adv., vol. 6, no. 19, May 2020, Art. no. eabb0451.
- [31] D. Luong, B. Balaji, and S. Rajan
Performance prediction for coherent noise radars using the correlation coefficient
IEEE Access, vol. 10, pp. 8627–8633, 2022.
- [32] S. S. Wilks
The large-sample distribution of the likelihood ratio for testing composite hypotheses
Ann. Math. Statist., vol. 9, no. 1, pp. 60–62, Mar. 1938.
- [33] R. R. Davidson and W. E. Lever
The limiting distribution of the likelihood ratio statistic under a class of local alternatives
Sankhyā: Indian J. Statist., Ser. A, vol. 32, no. 2, pp. 209–224, Jun. 1970.
- [34] G. W. Bohrnstedt and A. S. Goldberger
On the exact covariance of products of random variables
J. Amer. Stat. Assoc., vol. 64, no. 328, pp. 1439–1442, Dec. 1969.



David Luong (Graduate Student Member, IEEE) received the B.Sc. degree in mathematical physics from the University of Waterloo, Waterloo, ON, Canada, in 2013, and the M.Sc. degree in physics (quantum information) from the Institute for Quantum Computing, University of Waterloo, Waterloo, ON, Canada, in 2015, where he explored the practical aspects of quantum repeaters. He is currently working toward the Ph.D. degree in electrical and computer engineering with Carleton University, Ottawa, ON,

Canada.

From 2017 to 2020, he was a Defence Scientist with the Radar Sensing and Exploitation Section, Defence Research and Development Canada, Ottawa, where he helped develop a prototype microwave quantum radar. His research interests include quantum radar and signal processing.

Mr. Luong was awarded a Vanier Canada Graduate Scholarship in 2020, the highest scholarship awarded to Ph.D. students by the Canadian government.



Bhashyam Balaji (Senior Member, IEEE) received the B.Sc.(Hons.) degree in physics from St. Stephen's College, University of Delhi, New Delhi, India, in 1990, and the Ph.D. degree in theoretical particle physics from Boston University, Boston, MA, USA, in 1997.

Since 1998, he has been a Defence Scientist with Defence Research and Development Canada, Ottawa, ON, Canada. His research interests include quantum sensing (particularly quantum radar and quantum imaging); all aspects of

radar sensor outputs, including space-time adaptive processing, multitarget tracking, and meta-level tracking; and multisource data fusion. He has also applied quantum field theory methods, including Feynman path integrals, to the problems of nonlinear filtering and stochastic control.

Dr. Balaji was a recipient of the IEEE Canada Outstanding Engineer Award in 2018. He is a Fellow of the Institution of Engineering and Technology.



Sreeraman Rajan (Senior Member, IEEE) received the B.E. degree in electronics and communications from Bharathiyar University, Coimbatore, India, in 1987, the M.Sc. degree in electrical engineering from Tulane University, New Orleans, LA, USA, in 1992, and the Ph.D. degree in electrical engineering from the University of New Brunswick, Fredericton, NB, Canada, in 2004.

From 1986 to 1990, he was a Scientific Officer with the Reactor Control Division, Bhabha

Atomic Research Center (BARC), Mumbai, India, after undergoing intense training in nuclear science and engineering from its training school. At BARC, he developed systems for control, safety, and regulation of nuclear research and power reactors. During 1997–1998, he carried out research under a grant from Siemens Corporate Research, Princeton, NJ, USA. From 1999 to 2000, he was with JDS Uniphase, Ottawa, ON, Canada, where he worked on optical components and the development of signal processing algorithms for advanced fiberoptic modules. From 2000 to 2003, he was with Ceyba Corporation, Ottawa, where he developed channel monitoring, dynamic equalization, and optical power control solutions for advanced ultralong-haul and long-haul fiberoptic communication systems. In 2004, he was with Biopeak Corporation, where he developed signal processing algorithms for noninvasive medical devices. From December 2004 to June 2015, he was a Defence Scientist with the Defence Research and Development Canada, Ottawa. From July 2010 to June 2018, he was an Adjunct Professor with the School of Electrical Engineering and Computer Science, University of Ottawa, Ottawa, ON, Canada, and since July 2015, he has been an Adjunct Professor with the Department of Electrical and Computer Engineering, Royal Military College, Kingston, ON, Canada. In July 2015, he joined Carleton University as a Tier 2 Canada Research Chair (sensors systems) with the Department of Systems and Computer Engineering. From July 2015 to June 2020, he was an Associate Director of the Ottawa-Carleton Institute for Biomedical Engineering, Ottawa, and since July 2020, has been its Director. He is currently a Professor with the Department of Systems and Computer Engineering, Carleton University, Ottawa, ON, Canada. He holds two patents and two disclosures of invention. He has authored 200 journal articles and conference papers. His research interests include signal processing, biomedical signal processing, communication, and pattern classification.

Prof. Rajan was a recipient of the IEEE MGA Achievement Award in 2012 and of the Queen Elizabeth II Diamond Jubilee Medal in 2012 for his IEEE contributions. He was also a recipient of the 2016 W. S. Read Outstanding Service Award by IEEE Canada. He has been involved in organizing several successful IEEE conferences and has been a reviewer for several IEEE journals and conferences. He is currently the Chair of the IEEE Ottawa EMBS and AESS Chapters. He was a Board Member of IEEE Canada (2010–2018) and, since the beginning of 2021, he is the North America Region Director of the IEEE CTSoc.